Original Research Article

GREENHOUSE GASES SCIENCE AND TECHNOLOGY

Investigation on arsenopyrite dissolution and As (III) migration under geologic carbon storage conditions: A numerical simulation approach

Liwei Zhang, US Department of Energy, National Energy Technology Laboratory, Pittsburgh, PA, USA
Hariprasad Parthasarathy, Geosyntec Consultants, Greenville, SC, USA
Athanasios Karamalidis, Carnegie Mellon University, Pittsburgh, PA, USA

Abstract: Geologic carbon storage (GCS) is widely recognized as a promising strategy to reduce the emissions of greenhouse gas (GHG) to the atmosphere. However, the potential for mobilization of heavy metals, including arsenic (As), from their parent minerals in the subsurface because of induced dissolution due to carbon dioxide injection, remains a concern. In this study, A TOUGHREACT model was developed to investigate the potential of arsenopyrite dissolution in a deep arsenopyrite-rich formation in the presence of Fe(III)-bearing minerals under geologic carbon storage conditions (a CO_2 injection rate of 0.1 MMT/year, an average reservoir temperature of 50°C and an average reservoir pressure of 18.7 MPa). The model shows that after injection of CO_2, pH decreased as a result of CO_2 dissolution, which led to the release of $Fe^{3+}$from Fe(III)-bearing minerals. The oxidative Fe^{3+} released from the dissolution of Fe(III) bearing minerals caused dissolution of arsenopyrite and release of As(III). Therefore, dissolution of arsenopyrite is possible if Fe(III)-bearing minerals are present at or close to the arsenopyrite-rich formation. The model also simulated the rate of As(III) migration from the arsenopyrite-rich formation to a shallow aquifer above the formation. The As(III) migrated toward the shallow aquifer through a permeable borehole 23 m away from the CO_2 injector. Model simulations show that the As(III) contamination front migrated to 182 m above the As-rich layer at $t = 133$ days through the borehole given a CO_2 injection rate of 0.1 MMT/yr (3.17 kg/s), which corresponds to an average migration rate of 1.37 m/day. Model simulations also show that the rate of As(III) contamination front migration was not significantly affected by borehole permeability change. Those observations suggest that an aquifer, 1810 m above the As-rich layer as designed in model simulations, has the potential to be impacted by As contamination if an As-rich layer is present at or close to the CO_2 injection interval. It is important to note that this study investigates a worst-case scenario (from the

Correspondence to: Athanasios Karamalidis, Department of Civil and Environmental Engineering, 123L Porter Hall, Carnegie Mellon University, 5000 Forbes Ave, Pittsburgh, PA, 15213, USA. E-mail: akaramal@andrew.cmu.edu
Received June 22, 2016; revised October 27, 2016; accepted October 28, 2016
Published online at Wiley Online Library (wileyonlinelibrary.com). DOI: 10.1002/ghg.1651

perspectives of both site selection and abundance of arsenopyrite) and the results should not be interpreted as evidences making subsurface CO_2 storage projects unfeasible.

Supporting information is supplied as a separate online file for this article

Keywords: arsenopyrite dissolution; As(III) migration; geologic carbon storage; TOUGHREACT

Introduction

CO_2 concentration in the atmosphere has increased significantly since the advent of the industrial age,[1,2] and strategies to mitigate this problem have been investigated ever since. Among them, the most promising is geologic carbon storage (GCS). The strategy entails capture of CO_2 from large point sources of emission (e.g. coal-fired power plants) and storage in geologic carbon sinks.[2–4] Once injected in the geologic formation, the compressed CO_2 starts dissolving into the formation brine lowering the pH and could induce the release of metals and other constituents (e.g. organic compounds) from their parent minerals. This release could potentially result in the mobilization of naturally occurring contaminants.[5,6] For example, it is common to have arsenic (As) bearing minerals such as arsenopyrite (FeAsS), realgar (AsS), enargite ($CuAsS_4$), scorodite ($FeAsO_4{\cdot}2H_2O$), tennantite ($Cu_6[Cu_4(Fe,Zn)_2]As_4S_{13}$), and As_2S_3in the deep subsurface.[7,8] An analysis of rock samples taken from an aquifer deeper than 100 m at Zimapán Valley, México, shows an As content ranging from 10 to 10 500 mg/kg, depending on the location and rock type.[7] The primary sources of As in those rock samples are arsenopyrite, scorodite, and tennantite.[7] Therefore, an injection of CO_2 into a reservoir with As-bearing minerals may lead to the release of As from As-bearing minerals. In summary, due to relative abundance of As-bearing minerals in the environment and their occurrence in the lithophacies of GCS formations, there is a growing interest in the mechanism and kinetics of As release under GCS conditions. Exposure to As may have mild effects of human health, such as thickening and discoloration of the skin, stomach pain, nausea, vomiting, and several severe ones, such as causing cancer of the bladder, lungs, skin, kidney, nasal passages, liver, and prostate.[9]

A few numerical simulation and experimental studies were conducted to investigate the potential of As contamination in groundwater related to CO_2 injection into the subsurface. For example, Zheng *et al.*[6] conducted reactive transport simulations to evaluate to the extent of As mobilization in a shallow potable-water aquifer due to CO_2 intrusion and the involved mechanisms. The study suggested that oxidation of arsenian pyrite due to the presence of oxygen and other oxidative species, and desorption of As from clays and ferric oxyhydroxides, due to dissolution of clays and ferric oxyhydroxides as a result of CO_2 intrusion and pH drop, were two major mechanisms of As release. Viswanathan *et al.*[10] applied the reactive transport model developed by Zheng *et al.*[6] to evaluate As release potential at a CO_2 sequestration natural analog site in Chimayo, New Mexico. They concluded that although As can be released from dissolution of Fe-rich phases as a result of CO_2 intrusion, the released As adsorbs on the surface of illite, kaolinite, and smectite through surface complexation reactions, which decrease As concentration. Keating *et al.*[11] measured impacts of CO_2 dissolution on shallow groundwater quality in a sandstone aquifer in New Mexico, USA. They concluded that CO_2 is not mobilizing As, uranium, or lead from minerals within the shallow aquifer. Their geochemical model study suggested that the dissolution of calcite buffers against significant pH depression and may, therefore, inhibit mobilization of As, uranium, or lead. However, if CO_2 enters the shallow aquifer together with brackish water from deep formations, As contained in the brackish water may contaminate the aquifer.[11]

In this study, we investigated an As-bearing mineral dissolution scenario proposed by Parthasarathy *et al.*[12] that causes As release under GCS conditions, and a reservoir-scale numerical model was developed using two parameters from Parthasarathy *et al.*[12] to evaluate the impact of As release. Specifically, the dissolution rate constant of arsenopyrite ($10^{-8.09}$ mol/m^2/s) and the specific surface area of arsenopyrite (0.04 m^2/g) experimentally determined by Parthasarathy *et al.*[12] were used in this study. In Parthasarathy *et al.*[12] influent flow with dissolved Fe^{3+} concentration of

10^{-4} M went through a 5-cm long PEEK (Poly Ether Ether Ketone) column filled with arsenopyrite, and the dissolution rate of arsenopyrite was obtained by measuring dissolved As concentration at the effluent. The steady state arsenopyrite dissolution rates obtained at flow rates of 0.8 mL/min and 1.1 mL/min were calculated to be $10^{-8.09}$ mol/(m^2s). The BET surface area of the cleaned arsenopyrite particles were measured in triplicate using a 5-point Kr absorption isotherm and was found to be 0.04 ± 2% m^2/g.

Due to the relative abundance of arsenopyrite (FeAsS) under the reducing conditions predominant in most aquifers,[6,8] we choose arsenopyrite as the host mineral of As in this study. The process of As release from arsenopyrite is described as follows: (1) injected CO_2 lowers the pH and causes dissolution of iron-bearing minerals, which releases $Fe^{3+}$to solution; (2) Fe^{3+}causes oxidative dissolution of arsenopyrite, which results in release of $H_3AsO_3(aq)$ to solution. The dissolution reaction of arsenopyrite induced by Fe^{3+}can be written as:

$$FeAsS\ (s) + 5Fe^{3+}(aq) + 3H_2O \rightarrow 6Fe^{2+}(aq) + H_3AsO_3(aq) + S(s) + 3H^+(aq) \quad (1)$$

Based on this process, a numerical model was developed to determine the concentration of As released from arsenopyrite dissolution, and the rate of migration of released As toward shallow aquifers. Different from previous studies (As-bearing minerals are in or very close to shallow aquifers), the numerical model simulates a new scenario in which arsenopyrite is present in the CO_2 injection reservoir, and a migration pathway (like a leaky well, a natural fault or a borehole) connects the CO_2 injection reservoir with the shallow aquifer to allow potential migration of As from the CO_2 injection reservoir to the shallow aquifer. The scenario simulated in this study is a worst-case scenario, which has the As migration pathway very close to the CO_2 injection well to allow fastest migration of As from the CO_2 injection reservoir to the shallow aquifer.

Methodology

Reactive transport modeling

The reactive transport code TOUGHREACT[13] was used to simulate the geochemical reactions and transport process in a typical CO_2 injection scenario. TOUGHREACT is a numerical simulator to model coupled subsurface multiphase fluid and heat flow, solute transport, and chemical reactions.[14] TOUGHREACT was developed by introducing reactive transport into the existing framework of a non-isothermal, multi-component fluid and heat flow simulator TOUGH2.[15] TOUGHREACT has been previously used in applications that involve flow, transport, and complicated reaction networks, especially in the scenarios of carbon sequestration, enhanced oil recovery and groundwater remediation.[13,16–19]

Typical reactive transport formulation divides the chemical species into primary and secondary species, where the primary species define the chemistry of the system and the secondary species are written in terms of the primary species through the equilibrium constant expression of fast, instantaneous reactions.[20–22] The reactive transport of primary species is governed by mass conservation equation:[21]

$$\frac{d(\phi C_i)}{dt} = \underbrace{\frac{d}{dx}\left(\phi D_{ie}\frac{dC_i}{dx}\right)}_{\text{Diffusion term}} - \underbrace{\frac{d}{dx}(\phi u C_i)}_{\text{Advection term}} \pm \underbrace{\sum_{i=1}^{N} v_{ir}R_{ir}}_{\text{Reaction term}} \quad (2)$$

where ϕ is the porosity of the porous media (dimensionless), C_i is the concentration of species i (mol/m^3), D_{ie} is the effective diffusion coefficient of species i (m^2/s), u is flow velocity (m/s), R_{ir} is the rth reaction rate that can produce or consume species i (mol/m^3·s) and v_{ir} is stoichiometric number of species i in the rth reaction (dimensionless).

In the porous media, u is determined by Darcy's Law:

$$u = -\frac{k_{eff-w}}{\mu_w}(\nabla P_w - \rho_w g) \quad (3)$$

where $k_{eff\text{-}w}$ is the effective permeability of water in the formation which equals the product of the absolute permeability and the relative permeability of the liquid in the unit of m^2, μ_w is dynamic viscosity of water in the unit of Pa·S, $\nabla P_w$is pressure gradient in the unit of Pa/m, and $\rho_w g$ describes gravity effect in the unit of Pa/m.

The effective diffusion coefficient of species i (D_{ie}) in porous media can be calculated as:

$$D_{ie} = \phi\tau D_{iw} \quad (4)$$

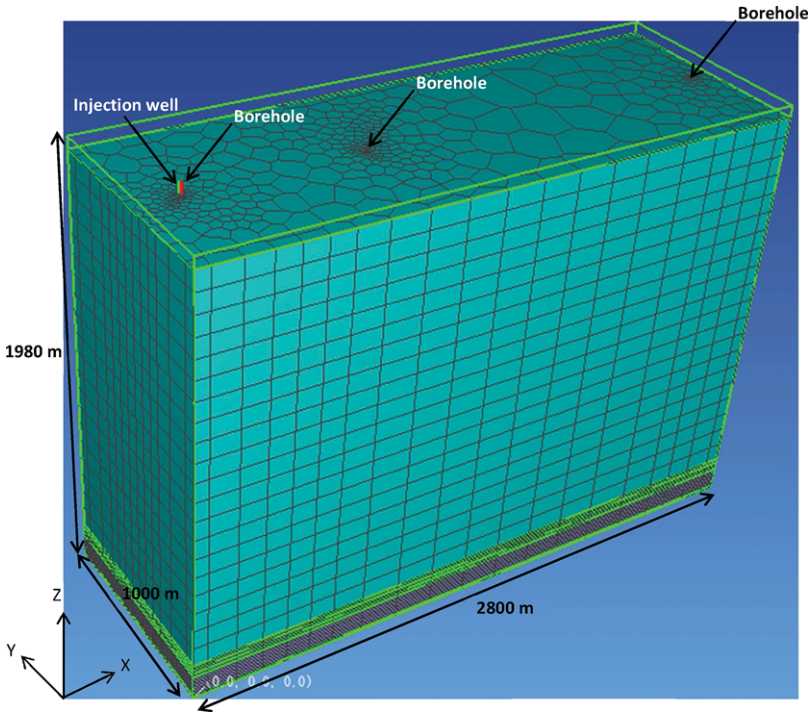

Figure 1. Dimensions of the modeling region.

where D_{iw} is the diffusion coefficient of species i in pure water, τ is the tortuosity of porous media, which is computed from $\tau = \phi^{1/3} S_w^{7/3}$, where S_w is water saturation.[14]

Model set-up

The TOUGHREACT model was constructed with six vertically stacked horizontal layers and the domain dimensions were 2800 m (D) × 1000 m (W) × 1980 m (H) (Fig. 1). Different layers have different physical and chemical properties. Physical and chemical properties of the six layers can be found in Tables 2 and 3. The top of the sixth layer (aquitard) is in contact with the shallow aquifer (20 m thick). The Fe_2O_3-rich layer was separated from the FeAsS-rich layer because the dissolution of Fe_2O_3 always causes dissolution of FeAsS, which means Fe_2O_3 and arsenopyrite cannot exist in the same layer and maintain a steady state. The FeAsS-rich layer was right above the Fe_2O_3-rich layer, which was designed to trigger maximum dissolution of FeAsS and that corresponded to the worst-case scenario. Brooks-Corey relative permeability function[23] was used to model relative permeability of brine and supercritical CO_2, and van Genuchten function[24] was used to model capillary pressure. The configuration of the six layers can be found in Fig. 2, and details of physical and chemical properties of each layer can be found in Tables 2 and 3.

The model simulated a 133 days CO_2 injection period with a constant CO_2 injection rate of 0.1 MMT/yr (3.17 kg/s), which was the CO_2 injection rate for pilot-scale CO_2 storage demonstration projects like Shenhua Ordos Carbon Dioxide Capture and Storage Project in Ordos (Inner Mongolia, China) and Kevin Dome Carbon Dioxide Capture and Storage Project in Northern Montana, USA.[25] A second model with an industrial scale CO_2 injection rate of 1 MMT/yr (31.7 kg/s) was also run. The CO_2 injection interval was from the top of Layer 1 to the bottom of Layer 3 (Fe_2O_3-rich layer). A relatively short CO_2 injection period was chosen in this study, because the primary goal of this study is to explore the potential of As release at deep subsurface under CO_2 storage conditions and migration of As from deep subsurface to a shallow aquifer, not to conduct a comprehensive study of As fate and transport in a long CO_2 injection period. The time step is greatly reduced to run the model to reach convergence with the increase of injection time, when more grid blocks become involved in reactive transport modeling with the propagation of CO_2 plume. Simulations that cover a long-time CO_2 injection period (e.g. 30 years) will be conducted in the

Table 1. Important reactive transport modeling parameters of quartz, hematite and arsenopyrite.

Mineral name	Dissolution/precipitation reactions	A_m(m^2/g)	Molar volume (cm^3/mol)	K_{eq} at 25 °C	k_m at 25 °C, (mol/(m^2s))	$\prod a_i^n$	E_a (kJ/mol)
Quartz (SiO_2)[a]	$SiO_2(s) \leftrightarrow SiO_2(aq)$	0.10	22.70	$10^{-3.74}$	$10^{-13.99}$	1.0	91.3
Hematite (Fe_2O_3)[b]	$Fe_2O_3(s) + 6H^+ \leftrightarrow 2Fe^{3+} + 3H_2O$	25.2	30.13	$10^{-0.04}$	$10^{-10.85}$	$[H^+]^{0.45}$	71.0
Arsenopyrite (FeAsS)[c]	$FeAsS(s) + 5Fe^{3+} + 3H_2O \leftrightarrow 6Fe^{2+} + H_3AsO_3 + S(s) + 3H^+$	0.04	26.83	$10^{41.55}$	$10^{-8.09}$	1.0	62.8

[a]Specific surface area of quartz is 0.1 m^2/g;[39] Molar volume of quartz is 22.70 cm^3/mol;[39] K_{eq} for quartz dissolution/precipitation is $10^{-3.74}$ at 25° C;[28] k_m for quartz dissolution/precipitation is $10^{-13.99}$ at 25 °C and $\prod a_i^n$ is 1.0;[40] E_a is 91.3 kJ/mol.[40]
[b]Specific surface area of hematite is 25.2 m^2/g (average of six hematite samples);[41] Molar volume of hematite is 30.13 cm^3/mol (calculated based on molecular weight of hematite (159.69 g/mol) and density of hematite (5.30 g/cm^3);[42] K_{eq} for hematite dissolution/precipitation is $10^{-0.04}$ at 25 °C;[43] k_m for hematite dissolution/precipitation is $10^{-10.85}$ at 25 °C and $\prod a_i^n$ is $[H^+]^{0.45}$;[44] E_a is 71.0 kJ/mol.[45]
[c]Specific surface area of arsenopyrite is 0.04 m^2/g;[12] Molar volume of arsenopyrite is 26.83 cm^3/mol (calculated based on molecular weight of arsenopyrite (162.83 g/mol) and density of arsenopyrite (6.07 g/cm^3));[42] K_{eq} for arsenopyrite dissolution/precipitation is $10^{41.55}$ at 25 °C (calculated based on ΔG_f value of FeAsS,[31] ΔG_f value of H_3AsO_3(aq)[30] and ΔG_f values of Fe^{3+} (aq), H_2O (l), Fe^{2+}(aq), S(s) and H^+ [29]). k_m for arsenopyrite dissolution/precipitation is $10^{-8.09}$ at 25° C and $\prod a_i^n$ is 1.0;[12] E_a is assumed to be the same as the default E_a value for minerals in TOUGHREACT (62.8 kJ/mol).[14]

future when a supercomputer is accessible, because it is important to mimic a long-term CO_2 injection scenario of a carbon capture and storage (CCS) site and to investigate the behavior of As migration in that scenario. The CO_2 injection well was located at X = 200 m and Y = 500 m, and the perforation zone of the well penetrated entire CO_2 storage formation (Fig. 3). A vertical borehole with high vertical permeability of 10^{-13} m^2 and a width of 16 m was located 23 m away from the injection well (Fig. 3), to create a worst-case scenario with an As leakage pathway very close to the injection well. Two other vertical boreholes that have the same properties as the first borehole were 800 m and 2500 m away from the injection well. The polygonal mesh was applied in this study and was automatically generated by TOUGHREACT, with the maximum individual cell area of 6×10^4 m^2. Small polygonal blocks were automatically generated in the regions close to the injection well and the boreholes by TOUGHREACT with the maximum individual cell area of 100 m^2, to capture complex two-phase transport and chemical reactions close to the injection well and the boreholes. The model had 19 018 active grid cells in total. Initial concentrations of aqueous species in Layers 1–6 can be found in Table 4. It is important to note that the concentrations of H^+, SiO_2 (aq), Fe^{2+}, Fe^{3+} and H_3AsO_3(aq) were equilibrium concentrations with the mineral phases in the sediments. The equilibrium concentrations were obtained from an equilibrium simulation using TOUGHREACT with no injection of CO_2.

Mineral dissolution and precipitation modeling – TST rate law

In this study, we use the TST (transition-state theory) rate law[26] to model all mineral dissolution and precipitation processes. The theory assumes a special type of chemical equilibrium (quasi-equilibrium) between reactants and activated transition state complexes, and the energy required for the reactants to be converted to activated transition state complexes is described by a term named activation energy.[27] The TST provides an approach to explain the temperature and concentration dependence of the reaction rate law. The TST rate law can be written as:[26]

$$R = A_m k_m \exp\left(-\frac{E_a}{RT}\right)\prod a_i^n\left(1-\exp\left(m_2 g^{m_3}\right)\right)^{m_1} \quad (5)$$

$$g = \frac{\Delta G}{RT} = \ln\left(\frac{Q}{K_{eq}}\right) \quad (6)$$

where A_m is the mineral surface area, km is the intrinsic rate constant in the unit of mol/m^2/s, E_a is the activation energy (kJ/mole) that describes temperature dependency of k_m, Q is the ion activity product for the

Table 2. Physical and chemical properties of Layers 1–6, as well as other model parameters.

Parameter	Value	Parameter	Value
Density of rock in Layers 1–6	2600 kg/m^3	CO_2 injection rate (constant rate)	0.1 MMT/year
Initial pressure at bottom of domain	19.5MPa	Brine residual saturation	0.2
Pressure gradient	9800 Pa/m	CO_2 residual saturation	0.1
Average CO_2 storage reservoir temperature	50°C	Brooks-Corey β	2
		van Genuchten 1/α	2×10^4 Pa
Horizontal permeability of Layers 1 and 5	10^{-19} m^2 (10^{-7} D)	van Genuchten λ	0.46
Vertical permeability of Layers 1 and 5	10^{-20} m^2 (10^{-8} D)	Boundary condition (horizontal and vertical-top)	Constant pressure and open boundary
Horizontal permeability of Layers 2, 3 and 4	10^{-12} m^2 (1 D)	Boundary condition (vertical-bottom)	closed boundary
Vertical permeability of Layers 2, 3, and 4	10^{-13} m^2 (0.1D)	EOS module used in TOUGHREACT	ECO2N
Horizontal permeability of Layer 6	10^{-16} m^2 (10^{-4} D)	Thickness of Layer 1	10 m
Vertical permeability of Layer 6	10^{-17} m^2 (10^{-5} D)	Thickness of Layer 2	100 m
Porosity of Layers 1 and 5	0.05	Thickness of Layers 3, 4 and 5	20 m for each layer
Porosity of Layers 2, 3, 4 and 6	0.2	Thickness of Layer 6	1790 m
Total simulation time	133 days	Horizontal permeability of borehole	10^{-12} m^2 (1 D)
Simulation time step	Automatic adjustment (initial step = 1000 s)	Vertical permeability of borehole	10^{-13} m^2 (0.1 D)
Rock compressibility	1.2×10^{-10} Pa^{-1}	Porosity of borehole	0.2

Table 3. Initial mineral composition in Layers 1–6.

Layer	Quartz (vol%)	Hematite (vol%)	Arsenopyrite (vol%)
Layer 1	100	0	0
Layer 2	100	0	0
Layer 3	99.0	1.0	0
Layer 4	99.99	0	0.01
Layer 5	100	0	0
Layer 6	100	0	0

mineral-water reaction, K_{eq} is the corresponding equilibrium constant, and $\prod a_i^n$ is a product representing the inhibitionor catalysis of the reaction by various ions in solution raised to the power n. In this study, we use a simplified form of the TST rate law, i.e., $m_1 = m_2 = m_3 = 1$. The simplified form of the TST rate law can be written as:

$$R = A_m k_m \exp\left(\frac{-E_a}{RT}\right)\prod a_i^n\left(1-\frac{Q}{K_{eq}}\right) \quad (7)$$

For simplicity, only three minerals (quartz, hematite, and arsenopyrite) were included in the reactive transport model. Specific surface areas, molar volumes, equilibrium constants (K_{eq}), dissolution/precipitation rate constants (k_m) and activation energy (E_a) of each mineral can be found in Table 1.

The correlation between K_{eq} and temperature (T) can be written as:

$$K_2 = exp\left[\left(\frac{-\Delta H_r^o}{RT_2} + \frac{\Delta H_r^o}{RT_1}\right) + LnK_1\right] \quad (8)$$

where K_2 is the equilibrium constant at T_2; $K_1$is the equilibrium constant at T_1 (usually T_1 equals to 298K); R is the gas constant; ΔH_r^o is the enthalpy of reaction.

For quartz, the correlation between K_{eq} and temperature (T, in the unit of K) can be written as:[28]

$$log_{10}\left(K_{eq-quartz}\right) = \frac{-1077.9}{T} - 0.1158 \quad (9)$$

For hematite, $\Delta H_r^o = 68.5$ kJ/mol (calculated based on H_f^o values of Fe_2O_3 (s), H_2O (l), H^+ and Fe^{3+} (aq).[29] Given $K_1$of $10^{-0.04}$ and $T_1 = 298$K,[28] the correlation between K_{eq} and temperature (T, in the unit of K) can be written as:

$$log_{10}\left(K_{eq-hematite}\right) = \frac{-3578}{T} + 11.97 \quad (10)$$

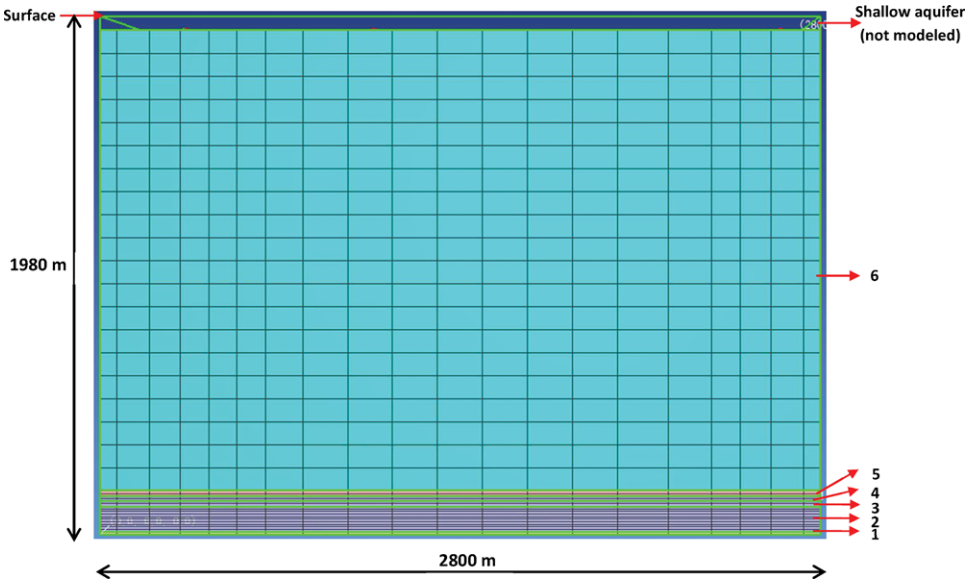

Figure 2. Configuration of 6 layers in the model. Layer 1: bottom of the domain (10 m thick); Layer 2: SiO_2 layer in the CO_2 storage formation (100 m thick); Layer 3: Fe_2O_3-rich layer in the CO_2 storage formation (20 m thick); Layer 4: arsenopyrite-rich layer in the CO_2 storage formation (20 m thick); Layer 5: caprock (20 m thick); Layer 6: aquitard (1790 m thick).

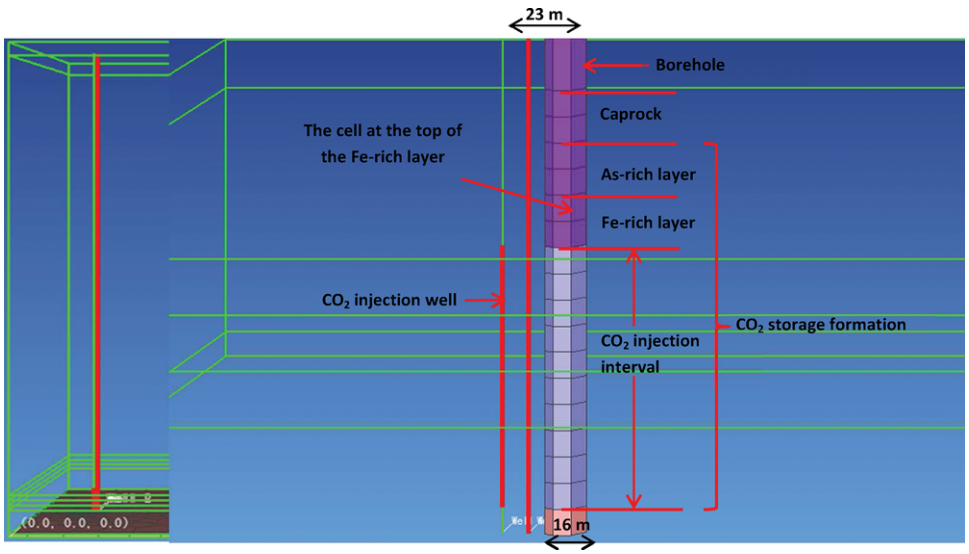

Figure 3. Zoom-in view of the injection well and the borehole.

For arsenopyrite, $\Delta H_r^o = -32.7$ kJ/mol (calculated based on H_f^o values of Fe^{2+} (aq), S(s), H^+, H_2O (l) and Fe^{3+} (aq);[29] H_f^o value of H_3AsO_3 (aq)[30] and H_f^o value of FeAsS[31]). Given K_1 of $10^{41.55}$ and $T_1 = 298$K,[28] the correlation between K_{eq} and temperature (T, in the unit of K) can be written as:

$$log_{10}\left(K_{eq-arsenopyrite}\right) = \frac{1707}{T} + 35.79 \qquad (11)$$

Results and discussion

Injection of CO_2 resulted in elevated CO_2 concentration near the injection well, and the region with high dissolved CO_2 concentration expanded with the increase of injection time (Fig. 4). At $t = 133$ days, maximum CO_2 concentration reached 3.21 wt% in the CO_2 storage formation, which approximately equaled to 0.73 mol CO_2/kg water. In TOUGHREACT, the

Table 4. Initial concentrations of aqueous species in Layers 1–6.

Aqueous species	Conc. in Layers 1–2 (mol/kg water)	Conc. in Layer 3 (mol/kg water)	Conc. in Layer 4 (mol/kg water)	Conc. in Layers 5–6 (mol/kg water)
Ca^{2+}	0.055	0.055	0.055	1.0×10^{-6}
Cl^{-}	0.36	0.36	0.36	6.1×10^{-6}
H^{+}	3.16×10^{-7}	2.0×10^{-7}	1.0×10^{-6}	3.16×10^{-7}
HCO_3^{-}	1.0×10^{-8}	1.0×10^{-8}	1.0×10^{-8}	1.0×10^{-8}
K^{+}	0.02	0.02	0.02	1.0×10^{-6}
Mg^{2+}	0.01	0.01	0.01	1.0×10^{-6}
Na^{+}	0.21	0.21	0.21	1.0×10^{-6}
SiO_2 (aq)	3.55×10^{-4}	3.50×10^{-4}	3.50×10^{-4}	3.1×10^{-4}
Fe^{2+}	1.0×10^{-15}	1.0×10^{-15}	1.8×10^{-6}	1.0×10^{-15}
Fe^{3+}	1.0×10^{-10}	4.25×10^{-7}	2.4×10^{-20}	1.0×10^{-10}
H_3AsO_3 (aq)	1.0×10^{-15}	1.0×10^{-15}	1.9×10^{-7}	1.0×10^{-15}

Note: For Layers 1, 2, 5 and 6, one mineral (quartz) is initially present in these layers. Therefore, the equilibrium concentration of SiO_2 (aq) (which is associated with dissolution of quartz) is calculated by TOUGHREACT. For Layer 3, two minerals (quartz and hematite) are initially present in that layer. Therefore, the equilibrium concentrations of SiO_2 (aq), H^+ and Fe^{3+} (which are associated with dissolution of quartz and hematite) are calculated by TOUGHREACT. For Layer 4, two minerals (quartz and arsenopyrite) are initially present in that layer. Therefore, the equilibrium concentrations of SiO_2 (aq), H^+, Fe^{2+}, Fe^{3+} and H_3AsO_3 (aq) (which are associated with dissolution of quartz and arsenopyrite) are calculated by TOUGHREACT.

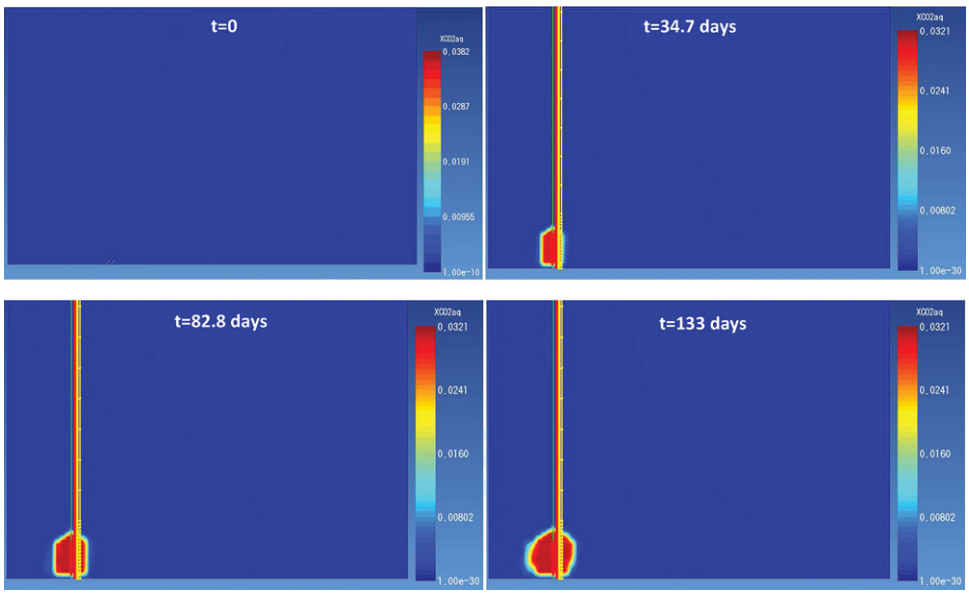

Figure 4. Dissolved CO_2 concentration (in the unit of mass fraction) near the injection well from t = 0 to t = 138.1 days.

solubility of CO_2 in water is calculated from the correlations specified in Spycher and Pruess.[32] For input parameters of temperature T and pressure P, these correlations obtain the compositions of coexisting CO_2 and brine phases and generally within experimental accuracy in the temperature range 12°C $\leq$ T $\leq$ 110°C, pressures up to 600 bar, and salinity up to saturated NaCl brines.[32] The high dissolved CO_2 concentration caused significant increase of $[H^+]$ near the injection well. At the top of the Fe-rich layer near

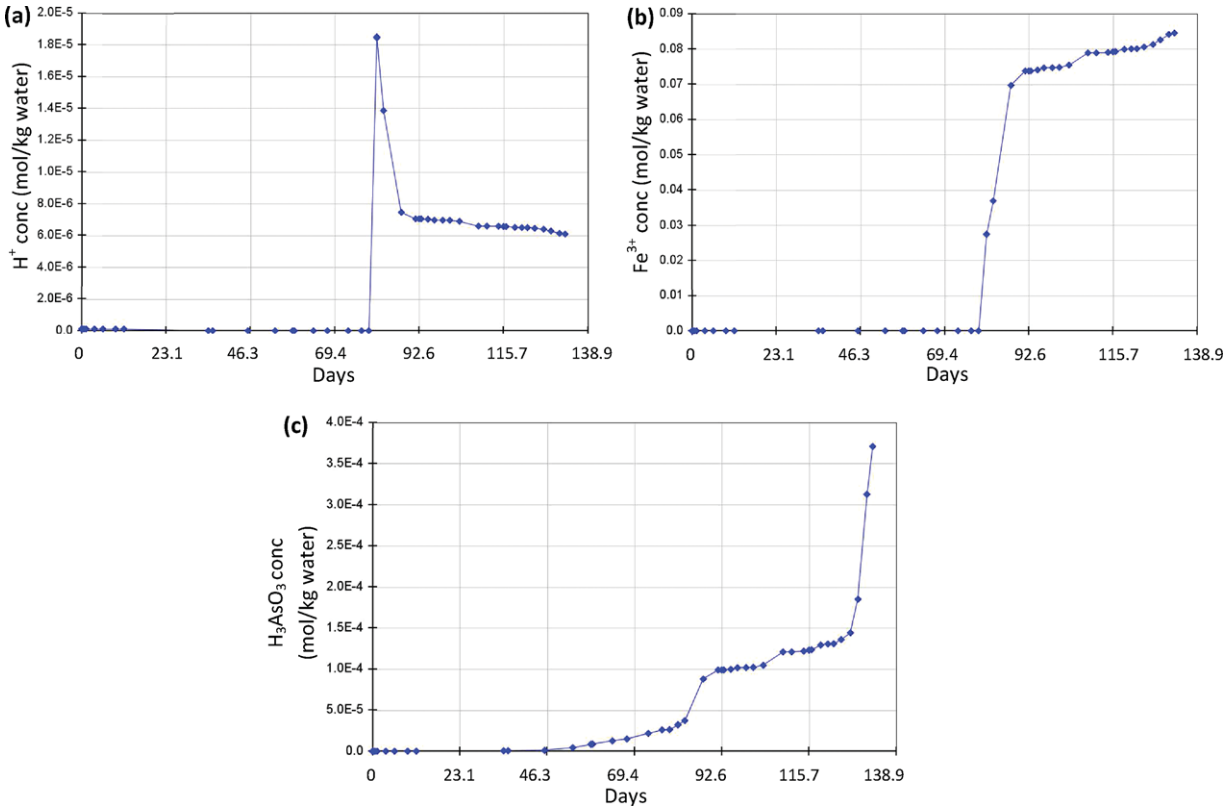

Figure 5. H+ concentration (a), Fe^{3+} concentration (b) and H_3AsO_3 (aq) concentration (c) at the top of the Fe_2O_3-rich layer (the location is marked in Figure 3) within the borehole from t = 0 to t = 133.1 days.

the injection well, the $[H^+]$ increases from initial value of 2.00×10^{-7} mol/kg water to 1.85×10^{-5} mol/kg water at $t = 81$ days due to an increase in dissolved CO_2 concentration. $[H^+]$ then slowly decreases from 1.85×10^{-5} mol/kg water to 6.00×10^{-6} mol/kg water at $t = 133$ days due to the consumption of H^+ to dissolve hematite (Fig. 5(a)).

The increase of $[H^+]$ near the injection well caused dissolution of hematite and subsequent increase of Fe^{3+} (aq) concentration in the Fe_2O_3-rich layer (Fig. 5(b)). Fe^{3+} (aq) from hematite dissolution migrated to the arsenopyrite-rich layer and caused oxidative dissolution of arsenopyrite (Fig. 5(c)). The maximum dissolved As concentration at the top of the Fe-rich layer reached 3.70×10^{-4} mol/kg water after 133 days of CO_2 injection, which equals to 27,721 ppb As. Although there are no maximum contaminants levels of As in deep brines, for reasons of comparison, the estimated value of As being released is 2772 times of the EPA drinking water As limit (10 ppb).[9]

Due to the existence of the highly permeable borehole (which serves as a leakage pathway) and the increase of the reservoir pressure induced by CO_2 injection, As will migrate upward along the borehole. Here we define the As contamination front as the location where the dissolved As concentration reaches Environmental Protection Agency (EPA) regulated maximum contamination level of 10 ppb, and the As contamination plume with the As contamination fronts as boundaries can be plotted by TOUGHREACT. The expansion of the plume and the distances of the As contamination front to the As-rich layer in vertical direction at different times can be seen in Fig. 6. At time = 0, the As concentration in the arsenopyrite-rich layer was high (1.9×10^{-7} mol/kg), because the As concentration was in equilibrium with arsenopyrite. Because of CO_2 injection, there was a movement of the As contamination front away from the arsenopyrite-rich layer and the moving distance of the As contamination front was positively correlated to the increase of CO_2 injection time.

Figure 7 shows the migration distance of the As contamination front as a function of time. The average As migration rate during this 133-day period was 1.37 m/day. For our system, the bottom of the shallow aquifer is 1810 m away from the As-rich layer.

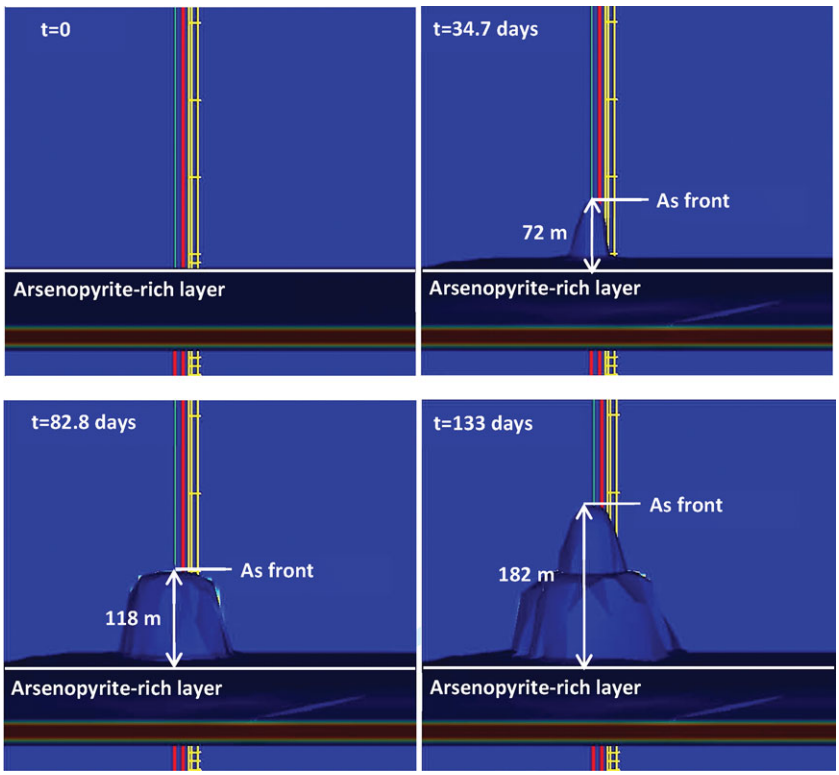

Figure 6. Expansion of the H_3AsO_3 (aq) plume showing the migration distance of the arsenic contamination front.

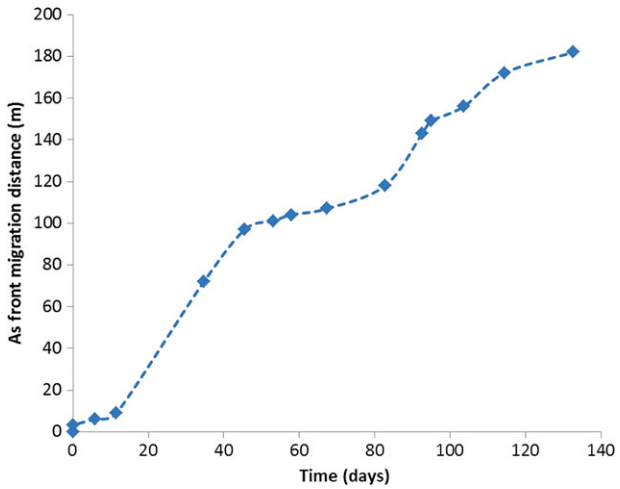

Figure 7. The migration distance of the arsenic contamination front as a function of time given a borehole vertical permeability of 10^{-13} m^2 and a CO2 injection rate of 0.1 MMT/year.

Therefore, if CO_2 keeps being injected and the As migration rate during the entire injection period remains at this value, it will take 3.6 years for the As contamination front to reach the shallow aquifer. As a result, there is a potential of As contamination at the shallow aquifer. Moreover, brine with As will continue to migrate upward after CO_2 injection stops. Even though pressure in the target formation may dissipate after injection stops, CO_2 may continue to rise up the borehole due to buoyancy forces, pushing brine into the aquifer at later times (Fig. S1 in the Supporting Information).

Figure 8 shows the migration distance of the As contamination front as a function of time, given different leakage pathway permeabilities (10^{-12} m^2, 10^{-13} m^2 and 10^{-14} m^2) and CO_2 injection rates. Results in Fig. 8 show that the rate of As(III) contamination front migration was not significantly affected by leakage pathway vertical permeability change. An explanation to those results is: the permeability of the leakage pathway determines the velocity of the advective brine flow in the leakage pathway, and the pressure difference (gravity force needs to be considered when calculating the pressure difference) between the two ends of the leakage pathway is the driving force for the upward advective

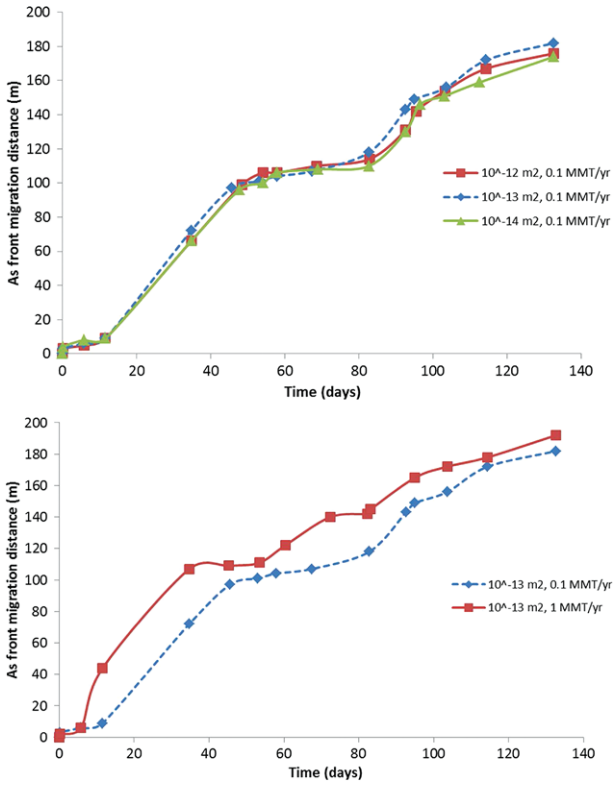

Figure 8. The migration distance of the arsenic contamination front as a function of time given different borehole vertical permeabilities (10^{-12} m^2, 10^{-13} m^2 and 10^{-14} m^2) and CO2 injection rates (0.1 MMT/year and 1 MMT/year).

flow. In this study, the injection rate of 0.1 MMT/yr CO_2 is not big, and thus the pressure gradient to drive the vertical flow of brine in the leakage pathway is relatively small. Therefore, As is able to migrate in horizontal directions in Fig. 6 and the horizontal movement of As reduces the amount of As moving upward. As a result, the change of leakage pathway vertical permeability does not have a significant impact on the migration rate of the As front. As for the impact of CO_2 injection rate on As migration, a higher CO_2 injection rate resulted in a faster As migration, because a higher CO_2 injection rate creates a higher pressure gradient to drive vertical brine flow in the leakage pathway, and the vertical brine migration will be accelerated by this higher pressure gradient.

This study assumes a worst-case scenario that allows maximum release of As, and the scenario does not consider the pH buffering effect of calcite and clay minerals in the CO_2 storage formation. The presence of pH buffering minerals like calcite and clay minerals in formation rocks can raise the pH of CO_2-rich reservoir porewaters.[33] Therefore, if the pH buffering effect of formation rocks is considered in our model, the pH of the Fe-rich layer may not decrease to 4.73 after 81 days of CO_2 injection. A higher pH means a lower dissolution rate of hematite and the dissolution rate of arsenopyrite will be lowered as well. Also, the presence of clay minerals in the CO_2 storage formation and the migration pathway allows sorption of As on the surface of clay minerals,[10] which may significantly reduce the migration rate of the As contamination front. A comprehensive geochemical model will be developed in the future to incorporate pH buffering and sorption effects. Moreover, in a real-world practice, appropriate site screening/characterization would certainly locate such a permeable borehole near the injection well and address that issue before any injection operations were initiated. It is also likely that an injection well location directly adjacent to a permeable borehole would not be selected. Therefore, though our observations suggest that a shallow aquifer has the potential to be impacted by As contamination in the worst-case scenario, those results should not be interpreted as evidences making subsurface CO_2 storage projects unfeasible.

To the best of our knowledge, this study is the first study to simulate As release in deep subsurface because of CO_2 injection and migration of As from deep subsurface to shallow aquifer. Other studies[6,10] simulated CO_2 migration from deep subsurface to shallow aquifer and mobilization of As caused by CO_2 dissolution at the shallow aquifer. Based on findings in this work and findings in Zheng *et al.*[6] and Viswanathan *et al.*[10] there is a chance of shallow aquifer contamination caused by As migration from deep subsurface to shallow aquifer, and it is possible to have the aquifer contaminated by As due to CO_2 migration into the aquifer and subsequent dissolution of As-rich minerals within the shallow aquifer.

Modeling limitations and implications

This study is a preliminary numerical simulation study to model subsurface As release under carbon sequestration conditions, and there are some limitations of this study.

(1) This study is a short-time simulation study with a total CO_2 injection period of 133 days. Long-time simulation is not achieved due to limited computational capacity. As a result, there is a desire

to get access to a supercomputer to run long-time simulations in the future. Simulations that cover a long-time CO_2 injection period (e.g. 30 years) are needed and will be conducted in the future because it is important to mimic a long-term CO_2 injection scenario of a CCS site and to investigate the behavior of As migration in that scenario.

(2) This study does not consider the complexity of mineral compositions in the CO_2 storage formation. Therefore, secondary carbonate and clay mineral formation during the CO_2 injection period is not included in the model. Impact of secondary carbonate and clay mineral formation on As mobility in deep subsurface is not well studied, and this issue is definitely worth investigating in the future.

(3) This study assumes a reductive environment (i.e., no oxygen is present and Fe(III) is the only oxidant to oxidize FeAsS in the model. Other processes that may cause As release under anoxic conditions such as interaction between arsenopyrite and $CaCl_2$[34] are not considered in this study. However, there is a potential for the injected CO2 to bring O2 (O2 is sometimes present in CO2 emitted from burning of fossil fuels[35,36]) to the CO2 storage formation, and O2 may accelerate the dissolution of FeAsS via the following reaction:[37]

$$FeAsS\,(s) + 3.5O_2 + 4H_2O \rightarrow Fe(OH)_3\,(s) + H_3AsO_4\,(aq) + 2H^+\,(aq) + SO_4^{2-}\,(aq) \quad (12)$$

Compared with Fe(III), O_2 is a stronger oxidant and the dissolution rate of FeAsS induced by O_2 is expected to be higher than the dissolution rate of FeAsS induced by Fe(III). Therefore, extra caution needs to be taken if the injected CO_2 contains O_2 and the target CO_2 storage formation contains As-bearing minerals.

(4) This study does not consider desorption of As from mineral surfaces in the subsurface. As discussed in Zheng *et al.*[6] and confirmed by Zheng *et al.*[38] desorption of As from mineral surfaces can release As to groundwater and potentially cause groundwater contamination. This study only considers dissolution of arsenopyrite, which may underestimate the amount of As released from formation parent rocks during the CO_2 injection period.

Conclusions

A reactive transport model is developed to simulate release of As from arsenopyrite near a CO_2 injection well and transport of As along a highly permeable borehole near the injection well. Simulation results show that dissolution of arsenopyrite is possible if Fe (III)-bearing minerals are close to the arsenopyrite-rich layer. Fe^{3+} released from Fe (III)-bearing minerals will cause dissolution of arsenopyrite and release of aqueous As, and release of Fe^{3+} is induced by low pH because of CO_2 injection. The increased reservoir pressure and rising of CO_2 plume in the borehole because of CO_2 injection may bring dissolved As upward and cause As contamination of the shallow aquifer. The As contamination front (where the As concentration reaches the EPA drinking water contamination level of 10 ppb) migrates to 182 m away from the arsenopyrite-rich layer at t = 133 days and if the As migration rate during a multi-year CO_2 injection period remains at this value, it will take 3.6 years for the As contamination front to reach the shallow aquifer 1810 m away from the deep arsenopyrite-rich layer. The rate of As contamination front migration is not significantly affected by borehole permeability change given a CO_2 injection rate of 0.1 MMT/yr. A higher CO_2 injection rate (i.e., 1 MMT/yr) results in a faster As migration than the scenario with a CO_2 injection rate of 0.1 MMT/yr. This study investigates a worst-case scenario and the results should not be interpreted as evidences making subsurface CO_2 storage projects unfeasible. Some issues (e.g. impact of residual O_2 in injected CO_2 and precipitation of secondary minerals) on mobility of As need to be investigated in the future.

Acknowledgements

This research was supported in part by an appointment to the National Energy Technology Laboratory Research Participation Program, sponsored by the US Department of Energy and administered by the Oak Ridge Institute for Science and Education. The authors would like to thank the Research and Innovation Center at NETL for funding support and providing access to research article databases, computing devices, etc. The authors also would like to thank Dr Robert Dilmore and Dr Yee Soong for their suggestions on boundary condition set-up and mesh refinement.

Disclaimer

References

1. Houghton JT, DingY, Griggs DJ, Noguer M, van der Winden PJ and Dai X, Climate Change 2001: The Scientific Basis. Contribution of Working Group 1 to the Third Assessment Report of the Intergovernmental Panel on Climate Change Cambridge, Cambridge University Press (2001).
2. Gasda SE, Bachu S and Celia MA, Spatial characterization of the location of potentially leaky wells penetrating a deep saline aquifer in a mature sedimentary basin. *Environ Geol* **46**(6–7):707–720 (2004).
3. Bachu S, Sequestration of CO_2 in geological media: Criteria and approach for site selection in response to climate change. *Energ Convers Manage* **41**:953–970 (2000).
4. Zhang L, Dzombak DA, Nakles DV, Brunet JPL and Li L, Reactive transport modeling of interactions between acid gas (CO_2+ H_2S) and pozzolan-amended wellbore cement under geologic carbon sequestration conditions. *Energ Fuel* **27**(11):6921–6937 (2013).
5. Kharaka YK, Cole DR, Hovorka S, Gunter WD, Knauss KG and Freifeld BM, Gas–water–rock interactions in Frio Formation following CO_2 injection: Implications for the storage of greenhouse gases in sedimentary basins. *Geology* **34**:577–580 (2006).
6. Zheng L, Apps JA, Zhang Y, Xu T and Birkholzer JT, On mobilization of lead and arsenic in groundwater in response to CO_2 leakage from deep geological storage. *Chem Geol* **268**(3):281–297 (2009).
7. Armienta MA, Villasenor G, Rodriguez R, Ongley LK and Mango H, The role of arsenic-bearing rocks in groundwater pollution at Zimapan Valley, Mexico. *Environ Geol* **40**(4–5):571–581 (2001).
8. Bose P and Sharma A, Role of iron in controlling speciation and mobilization of arsenic in subsurface environment. *Water Res* **36**(19):4916–4926 (2002).
9. US EPA. Arsenic Rule [Online]. US EPA (2014). Available at: http://water.epa.gov/lawsregs/rulesregs/sdwa/arsenic/regulations.cfm.
10. Viswanathan H, Dai Z, Lopano C, Keating E, Hakala A, Scheckel KG, *et al*., Developing a robust geochemical and reactive transport model to evaluate possible sources of arsenic at the CO_2 sequestration natural analog site in Chimayo, New Mexico. *Int J Greenhouse Gas Control* **10**:199–214 (2012).
11. Keating EH, Fessenden J, Kanjorski N, Koning DJ and Pawar R, The impact of CO_2 on shallow groundwater chemistry: observations at a natural analog site and implications for carbon sequestration. *Environ Earth Sci* **60**(3):521–536 (2010).
12. Parthasarathy H, Dzombak DA and Karamalidis AK, A small-scale flow-through column system to determine the rates of mineral dissolution at high temperature and pressure. *Chem Geol* **354**:65–72 (2013).
13. Xu T, Apps JA and Pruess K, Numerical simulation of CO_2 disposal by mineral trapping in deep aquifers. *Appl Geochem* **19**(6):917–936 (2004).
14. Xu T, Spycher N, Sonnenthal E, Zheng L and Pruess K, TOUGHREACT User's Guide: A Simulation Program for Non-isothermal Multiphase Reactive Transport in Variably Saturated Geologic Media, Version 2.0. Earth Sciences Division, Lawrence Berkeley National Laboratory, University of California, Berkeley, CA, USA (2012).
15. Pruess K, Oldenburg CM and Moridis GJ, TOUGH2 user's guide version 2. Earth Sciences Division, Lawrence Berkeley National Laboratory, University of California, Berkeley, CA, USA (1999).
16. Xu T, Apps JA and Pruess K, Mineral sequestration of carbon dioxide in a sandstone–shale system. *Chem Geol* **217**(3):295–318 (2005).
17. Vong CQ, Jacquemet N, Picot-Colbeaux G, Lions J, Rohmer J and Bouc O, Reactive transport modeling for impact assessment of a CO_2 intrusion on trace elements mobility within fresh groundwater and its natural attenuation for potential remediation. *Energ Procedia* **4**:3171–3178 (2011).
18. Shevalier M, Nightingale M and Mayer B, Comparison of a 2D Tough React model of CO_2 injection into a carbonate reservoir with chemical data from a CO_2 enhanced oil recovery project. *Proceedings of TOUGH Symposium 2012*, 17–19 (2012).
19. Brydie JR, Perkins EH, Fisher D, Girard M, Valencia M, Olson M and Rattray T, The development of a leak remediation technology for potential non-wellbore related leaks from CO_2 storage sites. *Energ Procedia* **63**:4601–4611 (2014).
20. Lichtner PC, Continuum model for simultaneous chemical reactions and mass transport in hydrothermal systems. *Geochim Cosmochim Acta* **49**(3):779−800 (1985).
21. Steefel CI and Lasaga AC, A coupled model for transport of multiple chemical species and kinetic precipitation/dissolution reactions with application to reactive flow in single phase hydrothermal systems. *Am J Sci* **294**:529−592 (1994).
22. Brunet JPL, Li L, Karpyn ZT, Kutchko BG, Strazisar B and Bromhal G, Dynamic evolution of cement composition and transport properties under conditions relevant to geological carbon sequestration. *Energ Fuel* **27**(8):4208–4220 (2013).
23. Brooks RH and Corey AT, Properties of porous media affecting fluid flow. *J Irr Drain Div-ASCE* **92**(2):61–90 (1966).
24. Van Genuchten MT, A closed-form equation for predicting the hydraulic conductivity of unsaturated soils. *Soil Sci Society Am J* **44**(5):892–898 (1980).
25. MIT, Carbon Capture and Sequestration Project Database [Online]. MIT (2015). Available at: https://sequestration.mit.edu/tools/projects/ [Accessed January 25, 2016].

26. Lasaga AC, Chemical kinetics of water-rock interactions, *J Geophys Res* **89**:4009–4025 (1984).
27. McNaught AD and Wilkinson A, *Compendium of Chemical Terminology: IUPAC Recommendations*, Blackwell Science, Oxford, UK (1997).
28. Wolery TJ, EQ3/6: Software Package for Geochemical Modeling of Aqueous Systems: Package Overview and Installation Guide (Version 8.0), Lawrence Livermore National Laboratory Report UCRL-MA-110662 PT I, Livermore, CA, USA (1992).
29. Haynes WM, CRC Handbook of Chemistry and Physics, 94th Edition, CRC Press, Boca Raton, FL (2013).
30. Henke K, Arsenic: Environmental Chemistry, Health Threats and Waste Treatment, John Wiley & Sons, Ltd, Chichester, UK (2009).
31. Pokrovski GS, Kara S and Roux J, Stability and solubility of arsenopyrite, FeAsS, in crustal fluids. *Geochim Cosmochim Acta* **66**(13):2361–2378 (2002).
32. Spycher N and Pruess K, CO_2-H_2O mixtures in the geological sequestration of CO_2. II. Partitioning in chloride brines at 12–100°C and up to 600 bar. *Geochim Cosmochim Acta* **69**(13):3309–3320 (2005).
33. Gherardi F, Audigane P and Gaucher EC, Predicting long-term geochemical alteration of wellbore cement in a generic geological CO_2 confinement site: Tackling a difficult reactive transport modeling challenge. *J Hydrol* **420**:340–359 (2012).
34. Parthasarathy H, Liu, H, Dzombak DA and Karamalidis AK, The effect of Na–Ca–Cl brines on the dissolution of arsenic from arsenopyrite under geologic carbon dioxide storage conditions. *Chem Geol* **428**:1–7 (2016).
35. Choi YS, Nesic S and Young D, Effect of impurities on the corrosion behavior of co_2 transmission pipeline steel in supercritical CO_2– water environments. *Environ Sci Technol* **44**(23):9233–9238 (2010).
36. Verba C, Potential impacts of formation waters on the integrity of class H cement and reservoir rock in carbon [co-] sequestration settings. PhD Dissertation, University of Oregon, Eugene, OR (2013).
37. Mukherjee S, *Applied Mineralogy: Applications in Industry and Environment*. Springer, Dordrecht, the Netherlands (2012).
38. Zheng L, Apps JA, Spycher N, Birkholzer JT, Kharaka YK, Thordsen J, *et al*., Geochemical modeling of changes in shallow groundwater chemistry observed during the MSU-ZERT CO_2 injection experiment. *Int J Greenhouse Gas Control* **7**:202-217 (2012).
39. Marty NCM, Tournassat C, Burnol A, Giffaut E and Gaucher EC, Influence of reaction kinetics and mesh refinement on the numerical modelling of concrete/clay interactions. *J Hydrol* **364**(1–2):58–72 (2009).
40. Carroll SA, McNab WW, Dai Z and Torres SC, Reactivity of Mount Simon sandstone and the Eau Claire Shale under CO_2 storage conditions. *Environ Sci Technol* **47**(1):252–261 (2012).
41. Cornell RM and Giovanoli R, Acid dissolution of hematites of different morphologies. *Clay Minerals* **28**:223–223 (1993).
42. Barthelmy D, Density of Minerals – Mineralogy Database [Online]. WebMineral (2014) Available at: http://webmineral.com/help/Density.shtml#.VhQoHMtVhBc [Accessed January 25, 2016].
43. Brgm. THERMODDEM: A thermodynamic database for modeling the alteration of wastes minerals [Online]. Brgm (2015). Available to: http://thermoddem.brgm.fr/data/mineraux.php [Accessed January 25, 2016].
44. Brantley SL, Ruebush S, Jang J and Tien M, Analysis of (bio) geochemical kinetics of Fe (III) oxides. *CMS Workshop Lectures* **14**:79 (2006).
45. Wells MA, Gilkes RJ and Fitzpatrick RW, Properties and acid dissolution of metal-substituted hematites. *Clays and Clay Minerals* **49**(1):60–72 (2001).

Liwei Zhang

Dr Liwei Zhang is an ORISE research associate at National Energy Technology Laboratory, U.S. DOE. He received his Ph.D. in Environmental Engineering from Carnegie Mellon University in 2013. His research areas are carbon storage, subsurface reactive transport modeling and shale gas development.

Hariprasad Parthasarathy

Dr Parthasarathy is an Environmental Engineer with Geosyntec Consultants, specializing in wastewater treatment design, data management, and geochemical modeling. He received his Ph.D. in Environmental engineering from Carnegie Mellon University in 2014, where his research focused on arsenic dissolution chemistry.

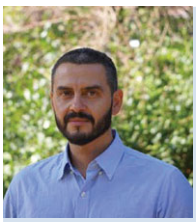

Athanasios K. Karamalidis

Dr Karamalidis is a professor at Associate Research Professor at Carnegie Mellon University. His current research interests include carbon storage and utilization, unconventional oil and gas development, and resource recovery with emphasis on development of new technologies and materials for the recovery of critical materials and rare earth elements.

